TMT Labeling Reveals the Effects of Exercises on the Proteomic Characteristics of the Subcutaneous Adipose Tissue of Growing High-Fat-Diet-Fed Rats

Ge Song, Junying Chen, Yimin Deng, Lingyu Sun, and Yi Yan*

Read Online

ACCESS | Metrics & More | Article Recommendations | SI Supporting Information

ABSTRACT: **Aim:** Growing period is an important period for fat remodeling. High-fat diet and exercise are reasons for adipose tissue (AT) remodeling, but existing evidence is not enough. Therefore, the effects of moderate-intensity continuous training (MICT) and high-intensity interval training (HIIT) on the proteomic characteristics of the subcutaneous AT of growing rats on normal diet or high-fat diet (HFD) were determined. **Methods:** Four-week-old male Sprague−Dawley rats ($n = 48$) were subdivided into six groups: normal diet control group, normal diet−MICT group, normal diet−HIIT group, HFD control group, HFD−MICT group, and HFD−HIIT group. Rats in the training group ran on a treadmill 5 days a week for 8 weeks (MICT: 50 min at 60−70% VO_{2max} intensity; HIIT: 7 min of warm-up and recovery at 70% VO_{2max} intensity, 6 sets of 3 min of 30% VO_{2max} followed by 3 min 90% VO_{2max}). Following physical assessment, inguinal subcutaneous adipose tissue (sWAT) was collected for proteome analysis using tandem mass tag labeling. **Results:** MICT and HIIT attenuated body fat mass and lean body mass but did not affect weight gain. Proteomics revealed the impact of exercise on ribosome, spliceosome, and the pentose phosphate pathway. However, the effect was reversed on HFD and normal diet. The differentially expressed proteins (DEPs) affected by MICT were related to oxygen transport, ribosome, and spliceosome. In comparison, the DEPs affected by HIIT were related to oxygen transport, mitochondrial electron transport, and mitochondrion protein. In HFD, HIIT was more likely to cause changes in immune proteins than MICT. However, exercise did not seem to reverse the protein effects of HFD. **Conclusion:** The exercise stress response in the growing period was stronger but increased the energy metabolism and metabolism. MICT and HIIT can reduce fat, increase muscle percentage, and improve maximum oxygen uptake in rats fed with HFD. However, in rats with normal diet, MICT and HIIT triggered more immune responses of sWAT, especially HIIT. In addition, spliceosomes may be the key factors in AT remodeling triggered by exercise and diet.
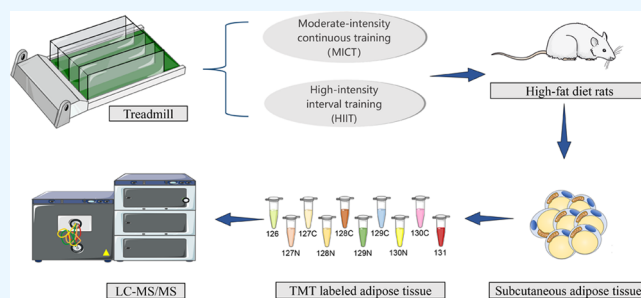
1. INTRODUCTION

The global prevalence of overweight and obesity is increasing remarkably and is also evident in children and adolescents.[1] High-fat diet (HFD) is an important risk factor for the disease and has greater temptation for children.[2,3] Thus, overweight and obese youths have much more risk of becoming overweight adults.[4]

Increasing physical activity benefits the health of children and young people,[5] and exercise plays an active role in the prevention and treatment of overweight and obesity.[6] Moderate-intensity continuous training (MICT) and high-intensity interval training (HIIT) are the most common forms of exercise intervention to improve the various biological processes of multiple organs[7−9] and prevent obesity,[10] but their effects and mechanisms are different.

The body's excess energy is stored in adipose tissue (AT) in the form of triglycerides. AT is considered one of the largest endocrine organs regulating obesity and other metabolic pathways.[11] Therefore, AT is an important target organ for studying the occurrence of overweight and obesity. However, AT distribution and function in different body compartments are different. Subcutaneous white adipose tissue (sWAT) plays a fundamental role in systemic glucose homeostasis and muscle metabolism.[12] Subcutaneous AT removal decreases glucose tolerance and insulin sensitivity in mice fed with HFD.[13] Moreover, subcutaneous AT relocation to the visceral cavity improves glucose tolerance in obese mice induced by HFD.[14] However, the angiogenic capacity of subcutaneous AT would be reduced by morbid obesity, resulting in insulin resistance and metabolic diseases.[15] In a word, subcutaneous AT plays a key role in obesity regulation.
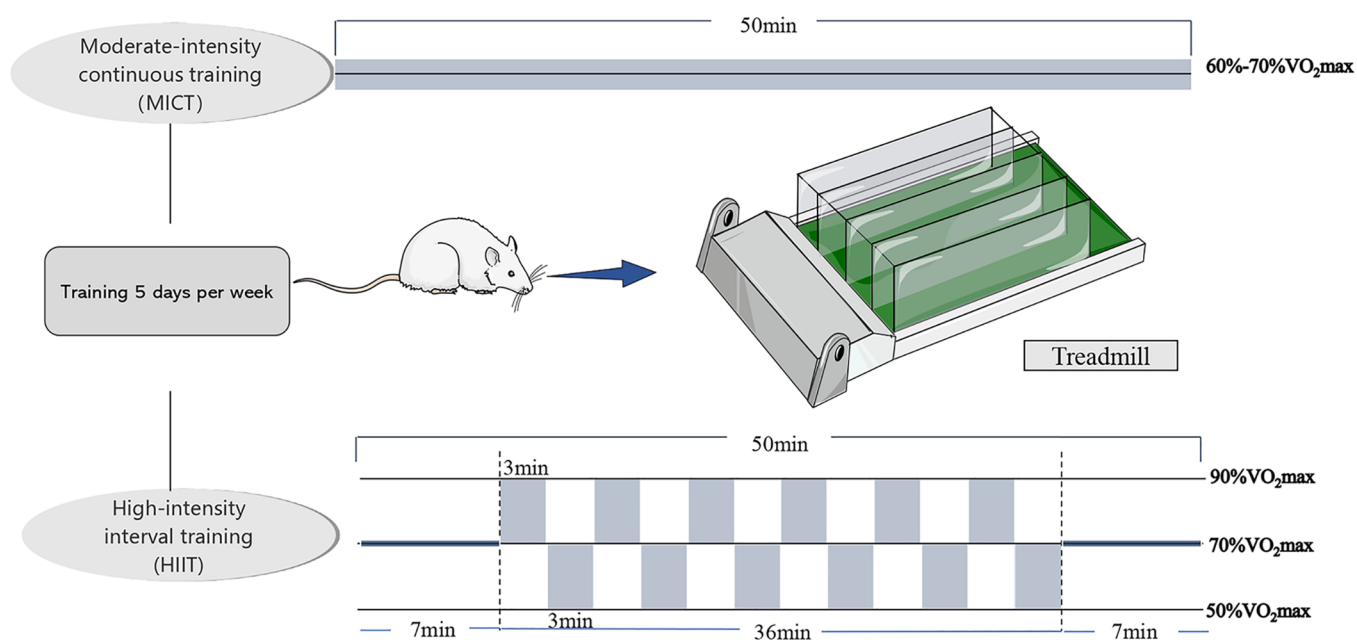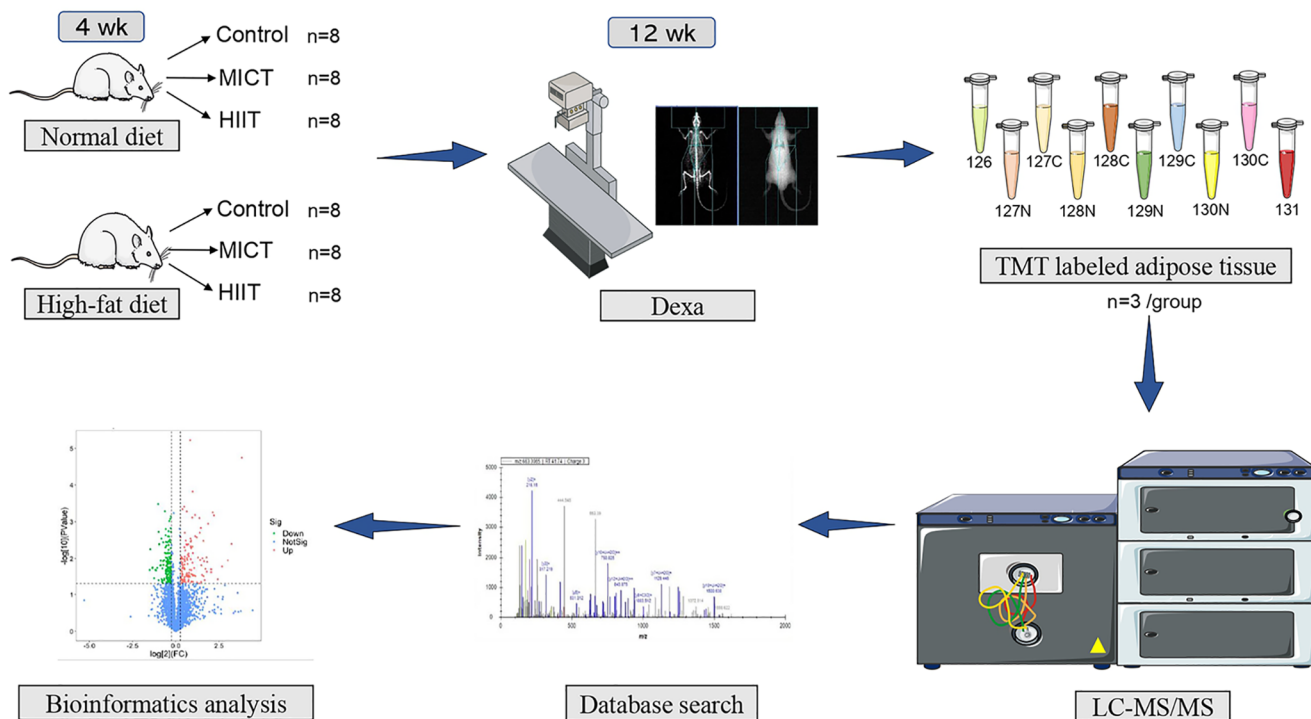
Figure 1. Experiment process. (A) Exercise intervention, (B) experiment process.

HFD and exercise (including HIIT and MICT) are reasons for AT remodeling, and they have opposite effects.[16−18] Although exercise is recognized for its health benefits in overweight or obese children, whether exercise can reverse the health damage of HFD, what type of exercise can correct nutritional remodeling, and the molecular mechanism is still unclear, especially for growing children.

Several studies have described the proteomic characteristics of white adipose tissue in mice or rats, but the high lipid content of adipose tissue, the difficulty of protein quantification, and the high number of biological repetitions of some experimental methods have limited the analysis of the overall protein changes in adipose tissue. We chose the method of TMT labeling to detect our samples. The 10-plex TMT method using

synchronous parent ion scanning in Orbitrap Fusion is very accurate and able to measure small expression differences in biological samples. And this is a method that has been used to great effect by others.[19−21] Exercise habits developed early in life can carry over into adulthood, providing lifelong health benefits.[22] Thus, the effects of 8-week MICT and HIIT on the proteomics of subcutaneous AT of growing rats in normal diet or HFD were observed to: (a) clarify the characteristics of MICT and HIIT on the proteomics of subcutaneous AT in growing rats in normal diet or HFD; (b) compare the effects of MICT or HIIT under different nutritional statuses on the proteomics of subcutaneous AT in growing rats; and (c) explore whether exercise could improve the metabolism of the subcutaneous AT of rats in HFD and which exercise model was much effective.

2. MATERIALS AND METHODS

2.1. Animals. The Animal Research Ethics Committee of Beijing Sport University (Beijing, China) approved the experiment protocols under license number 201937A. Forty-eight 3-week-old specific pathogen-free (SPF) weaning Sprague−Dawley rats were purchased from Beijing Weitongli-hua Laboratory Animal Co., Ltd., Beijing (License No. SCXK Beijing 2014-008). The animals were housed under standard SPF laboratory conditions (20−24 °C, 40−60% relative humidity, light: dark 12:12 h) and provided with pelleted food and water ad libitum.

After 1 week of adaptive feeding, the animals were randomly divided into normal diet control group (C, $n = 8$), normal diet−MICT group (CE, $n = 8$), normal diet−HIIT group (CH, $n = 8$), HFD control group (HC, $n = 8$), HFD−MICT group (HE, $n = 8$), and HFD−HIIT group (HH, $n = 8$). Groups C, CE, and CH were fed with control feed (3.82 kJ/g; 10% energy from fat, 20% from protein, and 70% from carbohydrate; Beijing Huafukang Biotechnology Co. Ltd., LOT No: D12451B); groups HC, HE, and HH were fed with high-fat feed with 45 kcal% fat (4.7 kJ/g; 45% energy from fat, 20% from protein, and 35% from carbohydrate; Beijing Huafukang Biotechnology Co., Ltd., LOT No: D12451) using the same formulation with D12451 from Research Diets.

2.2. Exercise Intervention. The training group received the exercise intervention for 8 weeks, 5 days a week. Rats of the CE and HE groups underwent 60−70% VO_{2max} intensity continuous treadmill training for 50 min. Before and after each training, the CH and HH groups were given 7 min each of warm-up and recovery treadmill training at 70% VO_{2max} intensity, followed by six sets of HIIT (3 min at 90% VO_{2max} + 3 min at 50% VO_{2max}) for a total of 50 min. VO_{2max} tests were performed every 2 weeks to calibrate speed (Figure 1).

2.3. Sample Selection. Sample collection was performed 48 h after the last exercise to avoid the effects of acute exercise. Dexa testing (XR-46, Norland) of body weight was performed prior to lethality. Rats were anesthetized with 10% chloral hydrate and then sacrificed by blood sampling from the abdominal aorta. Bilateral inguinal subcutaneous AT was collected and stored at −80 °C for subsequent testing. Finally, three rats from each group who completed the intervention process were randomly selected for tandem mass tag (TMT) proteomics testing.

2.4. TMT Proteomics. *2.4.1. Protein Extraction and Digestion.* The sample was dissolved in lysis buffer (7 M urea [Bio-Rad], 2 M thiourea [Sigma-Aldrich], and 0.1% CHAPS [Bio-Rad]). Then, the tissue was ground with three titanium dioxide abrasive beads (70 Hz, 120 s) followed by centrifugation at 5000g for 5 min at 4 °C. The supernatant was collected and

centrifuged at 15,000g for 30 min at 4 °C. The final supernatant was collected and stored at −80 °C until used. Total protein concentration was measured by the Bradford protein assay. Total protein (200 μg) from each sample was incubated at 55 °C for 1 h with 5 μL of 200 mM reducing reagent. Then, 5 μL of 375 mM iodoacetamide was added and incubated for 10 min at room temperature (RT) in the dark. Next, 200 μL of 100 mM dissolution buffer (AB Sciex) was added and centrifuged at 12,000g for 20 min. The sample was digested in trypsin for 14 h at RT, lyophilized, and redissolved with 100 mM dissolution buffer for labeling.

2.4.2. TMT Labeling. The TMT10plex reagent (Thermo Scientific, cat.#90111) was incubated at RT. Absolute ethyl alcohol (41 μL) was added to the TMT reagent (0.8 mg/tube) and mixed well. Because there were more samples than could be multiplexed in one TMT set, balanced batches were produced, and a common pool of all samples was also labeled and added to each batch. The TMT reagent (41 μL) was added to 100 μg of the digested sample. Then, the mixture was oscillated, centrifuged, incubated for 1 h at RT, and incubated in 5% quenching reagent (8 μL) for 15 min to terminate the reaction. The samples were stored after lyophilization. The efficiency of chemical tagging was 95%. TMT-labeled peptides were fractionated via basic reversed-phase chromatography on a RIGOL L-3000 dual-gradient high-performance liquid chromatograph (HPLC) using an Agela Durashell-C18 column (4.6 mm × 250 mm i.d., 5 μm, 100 Å). The column oven was set at 45 °C. Prior to loading peptides, the C18 column was washed with 100% methanol and equilibrated with Buffer A (0.1% ammonium hydroxide and 2% acetonitrile). Peptides were injected and eluted from the column using a gradient of mobile phase A (2% ACN, 0.1% NH_4OH) to mobile phase B (98% ACN, 0.1% NH_4OH) over 72 min at a flow rate of 0.7 mL/minute. The solvent gradient was set as follows: 5%B, 0 min; 5−8% B, 5 min; 8−18% B, 30 min; 18−32% B, 27 min; 32−95% B, 6 min; 95−5%, 4 min. The fractions collected were orthogonally concatenated into 10 pooled fractions.

2.4.3. Peptide Identification by Nano−Ultrahigh-Performance Liquid Chromatography (UPLC)−Tandem Mass Spectrometry (MS/MS). The acquired peptide fractions were suspended with 20 μL of buffer A (0.1% formic acid, 2% acetonitrile) and centrifuged at 12,000 rpm for 10 min. The supernatants (10 μL) were injected into the nano-UPLC−MS/MS system consisting of a Nanoflow high-performance liquid chromatography system (EASY-nLC 1000, Thermo Scientific) and an Orbitrap Fusion Lumos mass spectrometer (Thermo Scientific). The sample was loaded onto an Acclaim PepMap100 C18 column and then separated by an EASY-Spray C18 column (Beijing Qinglian Biotech Co., Ltd, China). Peptides were separated using a gradient from 6 to 12% B in 11 min, then 12−20% B in 37 min, and stepped up to 32% in 20 min followed by a 7 min wash at 95% B at 600 nL/min, where solvent A was 0.1% formic acid in water and solvent B was 80% ACN and 0.1% formic acid in water. The total duration of the run was 75 min. The mass spectrometer was operated in positive-ion mode (2.0 kV source voltage), and full MS scans were performed in the Orbitrap over the range of 300−1500 m/z at a resolution of 120,000 with an automatic gain control (AGC) target of 4e^5 and a maximum ion injection time of 50 ms. The scan range was 350−1550 m/z. Following higher-energy collisional dissociation (HCD) with a normalized collision energy (NCE) of 32%, MS/MS spectra were collected in the Orbitrap (60,000 resolution) with an AGC target of 5e^4 and a maximum ion injection time of
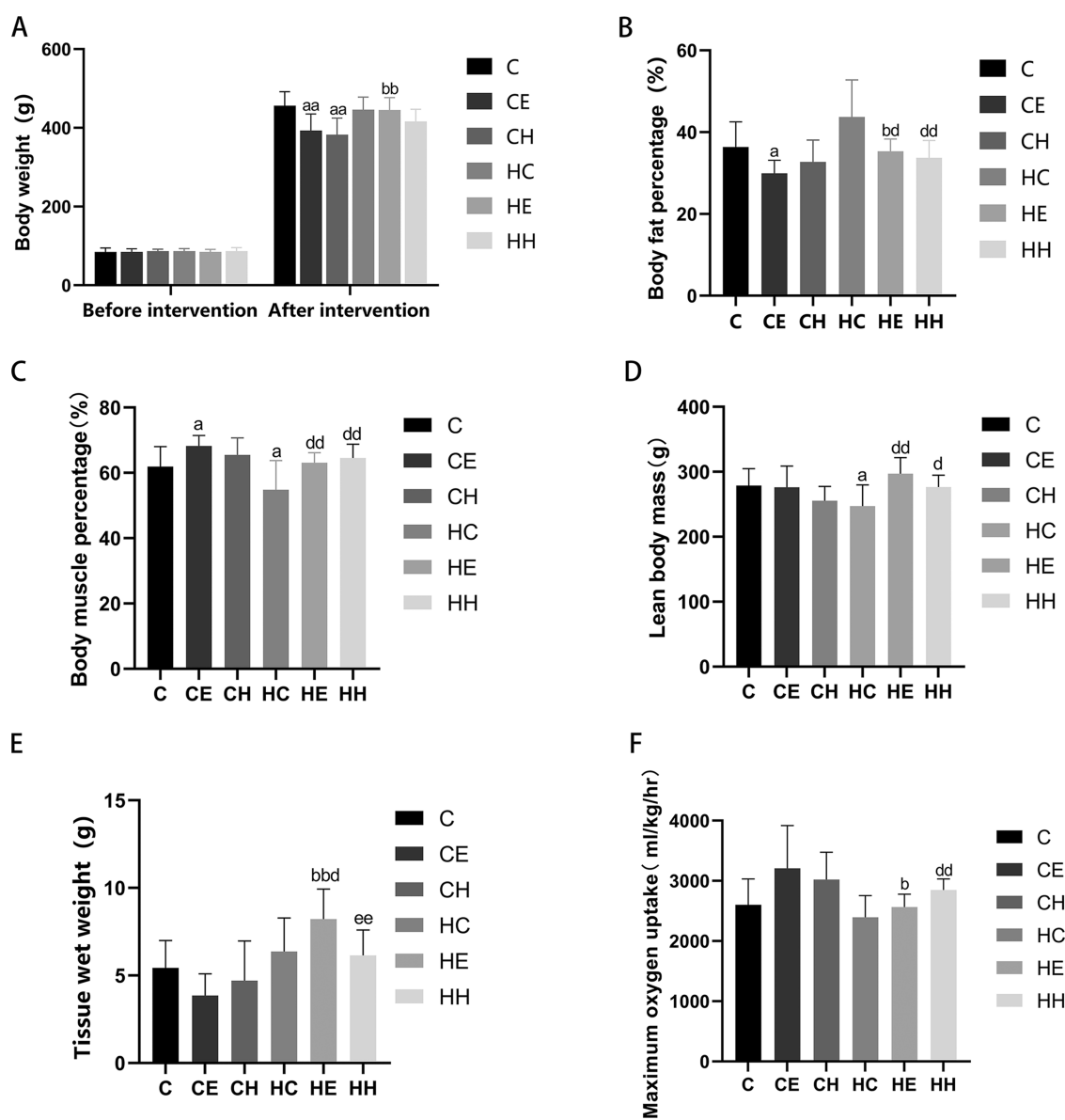
Figure 2. Physical characteristics of animals. (A) Body weight, (B) body fat percentage, (C) body muscle percentage, (D) lean body mass, (E) bilateral inguinal subcutaneous AT wet weight, (F) maximum oxygen uptake. $^{a}P < 0.05$, compared with C group; $^{b}P < 0.05$, $^{bb}P < 0.01$, compared with CE group; $^{d}P < 0.05$, $^{dd}P < 0.01$, compared with HC group; $^{e}P < 0.05$, $^{ee}P < 0.01$ compared with HE group.

118 ms. The database used in this experiment is the Uniprot_RAT database. The resulting MS/MS data were processed using Proteome Discoverer 2.1.

2.4.4. Protein Identification. Identification was set as follows: fully tryptic specificity, maximum of two missed cleavages, minimum peptide length of 6, fixed modifications for TMT tags on lysine residues and peptide N-termini (+229.162932Da), and carbamidomethylation of cysteine residues (+57.02146Da), variable modifications for oxidation of methionine residues (+15.99492Da), precursor mass tolerance of 15 ppm and a fragment mass tolerance of 0.02 Da for MS2 spectra collected in the Orbitrap. A percolator was used to filter peptide spectral matches and peptides to a false discovery rate (FDR) of less than 1%. After spectral assignment, peptides were assembled into proteins and were further filtered based on the combined probabilities of their constituent peptides to a final FDR of 1%. Only unique and razor peptides were considered for quantification.

2.4.5. Bioinformatics Analysis. C2 gene sets from Molecular Signatures Database Collections (c2.cp.kegg.v7.5.symbols.gmt) identified the proteome signatures enriched in CE versus C and CH versus C using the Gene Set Enrichment Analysis (GSEA) software (v4.2.1). The criteria of differentially expressed proteins (DEPs) were fold change >1.5 or <0.67, and $P < 0.05$ was considered statistically significant. In this study, the Gene Ontology (GO) terms and Kyoto Encyclopedia of Genes and Genomes (KEGG) pathway enrichment analysis of DEPs were automatically completed and visualized by clusterProfiler version 4.3.0 in R software.

2.5. Western Blot Validation. Total proteins were extracted with RIPA buffer, and the protein concentration was determined using the BCA protein assay kit. Equal amounts of protein (20−40 μg) were resolved on SDS-PAGE gels and then transferred to PVDF membranes. The following antibodies were used: β-actin (mouse antibody; 1:2000 dilution; CWbio, Taizhou, China); Pfkp (rabbit antibody; 1:500 dilution;
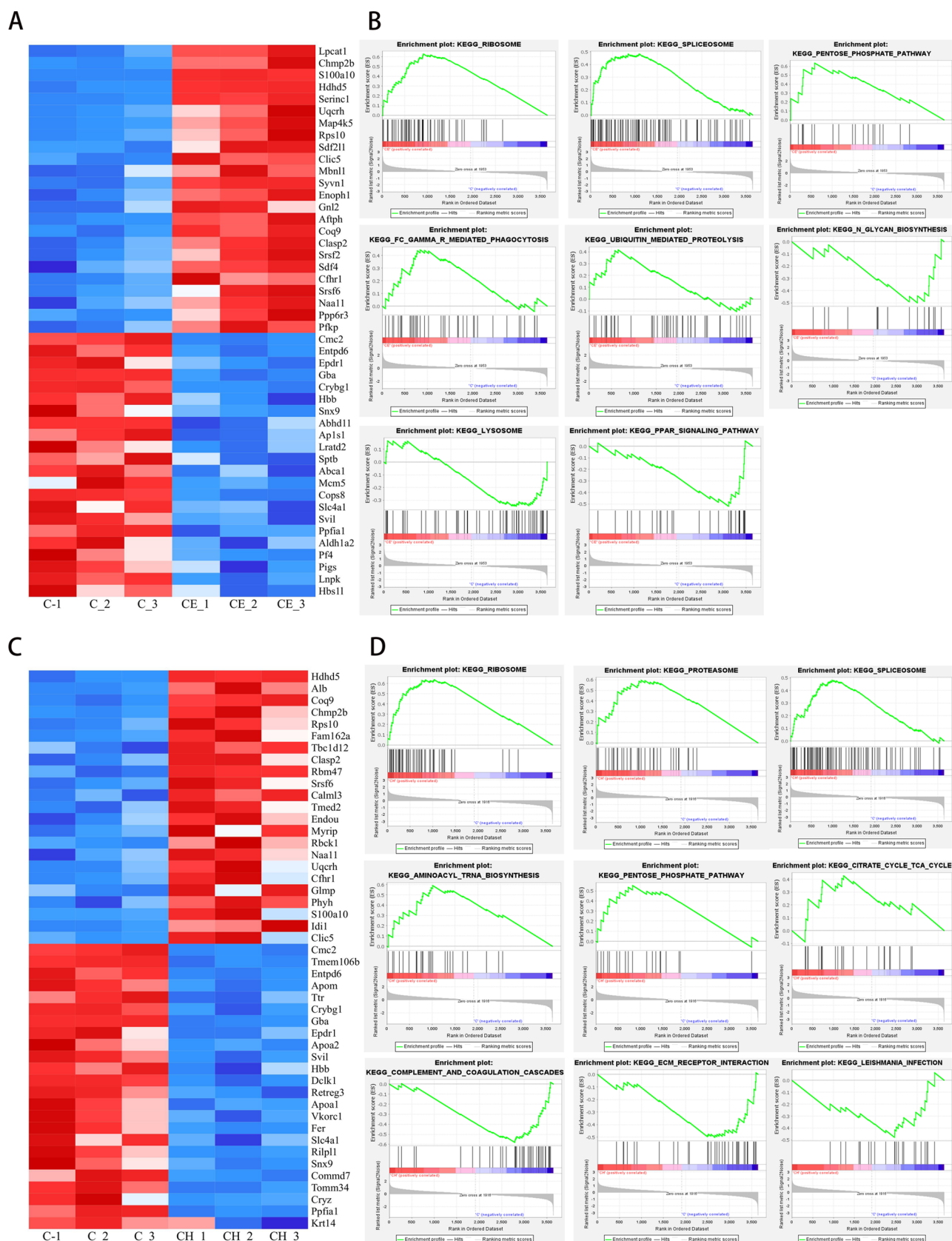
Figure 3. GSEA enrichment in the normal diet group. (A) Left is a heatmap of the top 50 proteins in CE versus C. Red means upregulation, and blue means downregulation. (B) Pathways with significant differences in CE versus C. (C) Left is a heatmap of the top 50 proteins in CH versus C. (D) Pathways with significant differences in CH versus C.
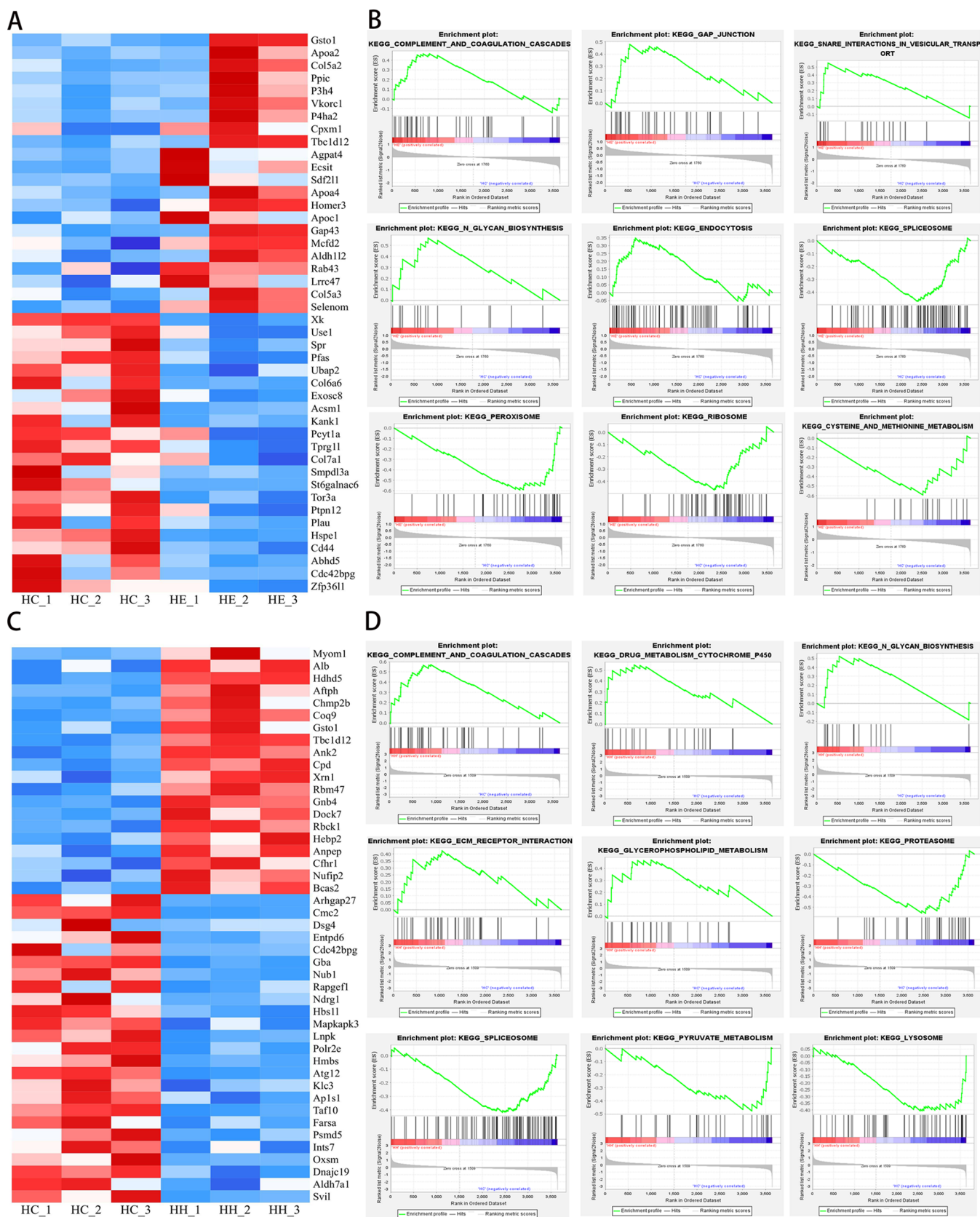
Figure 4. GSEA enrichment in the HFD group. (A) Heatmap of the top 50 proteins in HE versus HC. (B) Pathways with significant differences in HE versus HC. (C) Heatmap of the top 50 proteins in HH vs HC. (D) Pathways with significant differences in HH versus HC.

Proteintech, Wuhan, China); Crp (rabbit antibody; 1:2000 dilution; Proteintech, Wuhan, China); Fasn (rabbit antibody; 1:1000 dilution; Cell Signaling Technology, Boston). The membranes were then incubated with anti-rabbit or anti-mouse
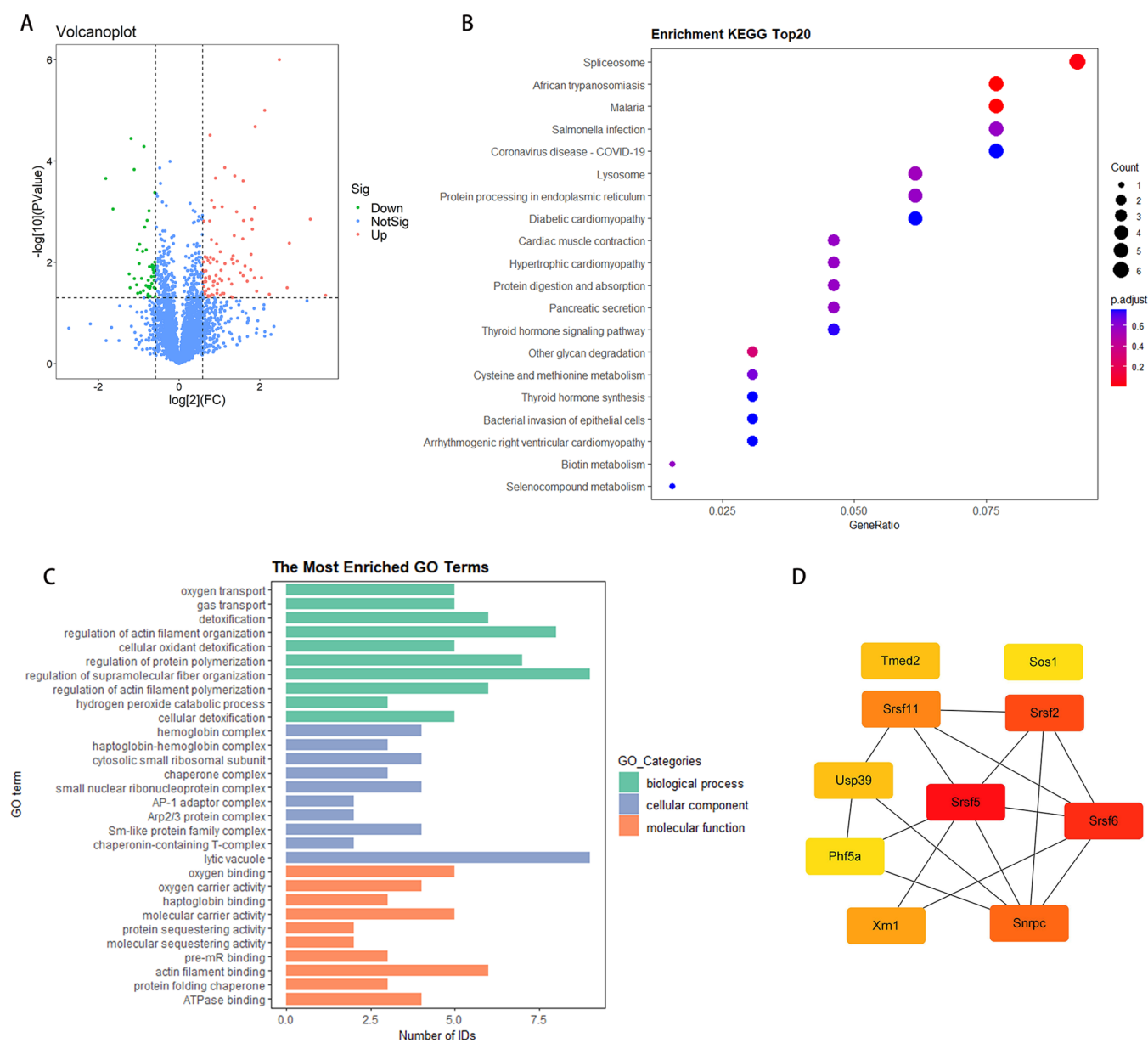
Figure 5. Functional correlation analysis of DEPs in CE versus C. (A) Volcano map of DEPs in CE versus C. (B) KEGG analysis in CE versus C. The x-axis label represents gene ratio, and the y-axis label represents the KEGG pathway. The size of the dot indicates the amount of genes under a specific term, and the color of the dot indicates the P-value. (C) GO function annotation analysis in CE versus C. (D) Top 10 hub genes of PPI in CE versus C. The redder the color, the higher the MCC score.

IgG HRP-conjugated secondary antibodies. The bands were visualized with enhanced chemiluminescence (ECL) reagents and analyzed using the Chemi-Doc System (Bio-Rad). The levels of target proteins were normalized against the β-actin protein levels. Band intensities were measured using ImageJ software (NIH).

2.6. Statistical Analyses. Statistical analyses were performed in SPSS 22.0 and visualized in GraphPad Prism version 8.0 (GraphPad Software, San Diego, CA). Two-factor ANOVA was used for body weight, body fat percentage, lean body mass, skeletal muscle percentage, and maximum oxygen uptake. The material in Figure 1 is from https://smart.servier.com/.

3. RESULTS

3.1. Physical Characteristics of Animals. Before the start of the experiment, we ensured that the body weights of rats in

each group had no remarkable differences (Figure 2A). After 8 weeks of intervention, the HFD-fed rats showed a much poorer haircoat quality. MICT and HIIT reduced the body weight of normal-diet-fed rats ($P < 0.01$), but no significant differences were found in HFD-fed rats ($P > 0.05$). However, as expected, the body fat percentages of rats in the HE and HH groups were significantly lower than that in the HC group ($P < 0.01$), and the lean body weight ($P < 0.05$) and the body muscle percentage of ($P < 0.01$) in the HE and HH groups were significantly higher than those in the HC group (Figure 2B−D). In addition, the wet weight of subcutaneous AT was also measured. The tissue weight in the HE group was remarkably higher than that in the CE group, and surprisingly, the subcutaneous AT of rats in the HE group was heavier than that in the HC group (Figure 2E). Before the intervention, the VO_{2max} values of rats in different groups had no remarkable differences. After the intervention, the
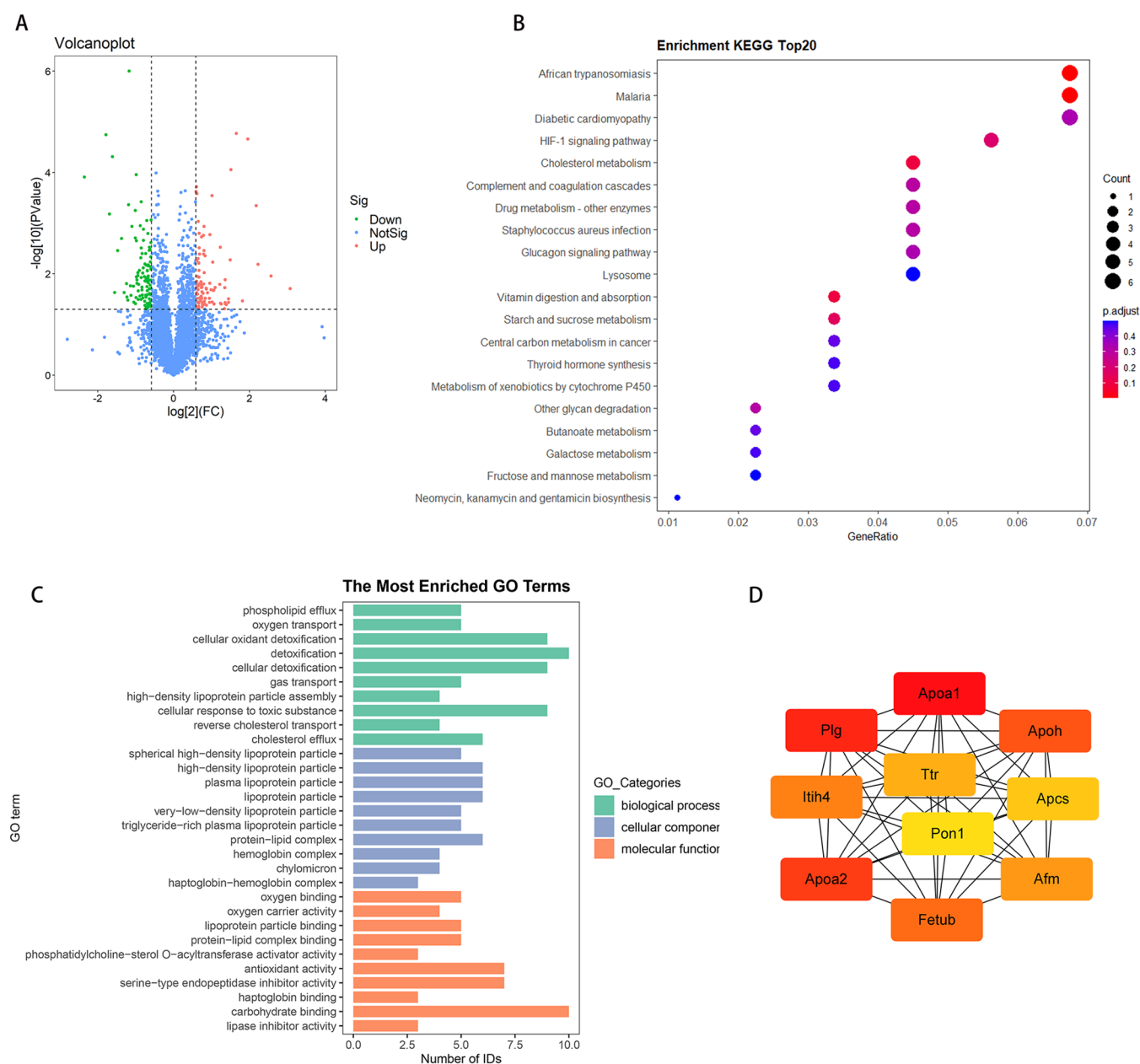
Figure 6. Functional correlation analysis of DEPs in CH versus C. (A) Volcano map of DEPs in CH versus C. (B) KEGG analysis in CH versus C. (C) GO function annotation analysis in CH versus C. (D) Top 10 hub genes of PPI in CH versus C. The redder the color, the higher the MCC score.

VO_{2max} in the exercise groups was higher than that in the control groups under the same diet intervention. Only the HFD group had a statistically different VO_{2max}. The HFD group had lower VO_{2max} than the normal diet group even with MICT.

3.2. GSEA Reveals the Effects of MICT and HIIT on AT. A total of 4265 individual proteins were identified and quantified in total in this study. GSEA was carried out to identify the effects and mechanisms of different exercise modes on AT. The analysis indicated that the dataset has 3645 genes for CE versus C comparison. A total of 1953 highly expressed genes were found in the CE group with a correlation area of 58.0%, and 1692 genes were highly expressed in the C group with a correlation area of 42.0%. The most significantly enriched gene sets positively correlated with the CE group included ribosome, spliceosome, pentose phosphate pathway (PPP), Fc γ R-mediated phagocytosis, and ubiquitin-mediated proteolysis ($P < 0.05$). The most significantly enriched gene sets negatively correlated with

the CE group included PPAR signaling pathway, N-glycan biosynthesis, and lysosome ($P < 0.05$, Figure 3A,B).

A total of 3645 genes were identified in the CH versus C comparison, 1916 genes were highly expressed in the CH group with a correlation area of 52.7%, and 1729 genes were highly expressed in the C group with a correlation area of 47.3%. The most significantly enriched gene sets positively correlated with the CH group included ribosome, proteasome, spliceosome, aminoacyl tRNA biosynthesis, pentose phosphate pathway, citrate cycle, and tricarboxylic acid cycle ($P < 0.05$). The most significantly enriched gene sets negatively correlated with the CH group included complement and coagulation cascades, extracellular matrix (ECM)−receptor interaction, and leishmania infection ($P < 0.05$, Figure 3C,D).

The analysis indicated that the dataset has 3645 genes for the HE versus HC comparison. A total of 1760 highly expressed genes were found in the HE group with a correlation area of
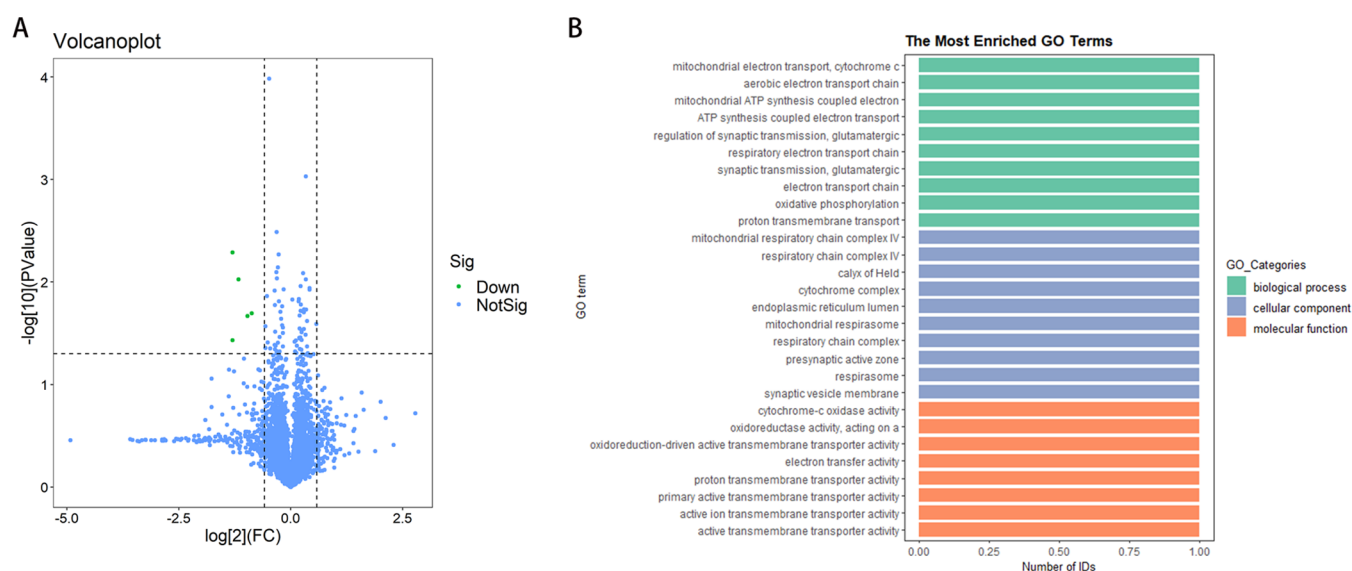
Figure 7. Functional correlation analysis of DEPs in HE versus HC. (A) Volcano map of DEPs in HE versus HC. (B) GO function annotation analysis in HE versus HC.

44.9%, and 1885 genes were highly expressed in the HC group with a correlation area of 55.1%. The most significantly enriched gene sets positively correlated with the HE group included complement and coagulation cascades, gap junction, snare interactions in vesicular transport, N-glycan biosynthesis, and endocytosis ($P < 0.05$). The most significantly enriched gene sets negatively correlated with the HE group included spliceosome, peroxisome, proteasome, ribosome, and cysteine and methionine metabolism ($P < 0.05$, Figure 4A,B).

A total of 3645 genes were also obtained in the HH versus HC comparison. A total of 1509 genes were highly expressed in the HH group with a correlation area of 42.7%, and 2136 genes were highly expressed in the HC group with a correlation area of 57.3%. The most significantly enriched gene sets positively correlated with the HH group included complement and coagulation cascades, drug metabolism cytochrome p450, N-glycan biosynthesis, ECM–receptor interaction, glycerophospholipid metabolism, and chemokine signaling pathway ($P < 0.05$). The most significantly enriched gene sets negatively correlated with the HH group included proteasome, spliceosome, lysosome, aminoacyl tRNA biosynthesis, pyruvate metabolism, valine, leucine and isoleucine degradation, pyrimidine metabolism, and cysteine and methionine metabolism ($P < 0.05$, Figure 4C,D).

3.3. Functional Correlation Analysis of DEPs in a Normal Diet. A total of 139 proteins were differentially abundant between groups, among which 88 were upregulated and 51 were downregulated in the CE group compared with C group sWAT (Figure 5A). GO function annotation analysis showed that the DEPs affected by MICT were related to hemoglobin complex, which influenced oxygen transport and oxygen carrier activity (Figure 5C). KEGG also showed that spliceosome and lysosome were enriched remarkably (Figure 5B). The DEPs were sorted according to P value. The most significantly altered proteins in CE versus C were involved in the neuromuscular process (Mycbp2, Gba) and endoplasmic reticulum (Gba, Lnpk, S100a10, Syvn1; Table S1). The maximal clique centrality (MCC) method of the CytoHubba plug-in in Cytoscape was used to screen the top 10 hub genes. The hub

genes were associated with spliceosome (Srsf 2, Srsf 5, Srsf 6, and Srsf 11; Figure 5D).

A total of 204 DEPs (99 upregulated and 105 downregulated) were identified in the CH group compared with the C group (Figure 6A). GO functional annotation analysis showed that the DEPs affected by HIIT were related to lipoprotein particle, as well as biological processes and molecular functions involved in oxygen transport and oxygen carrier activity (Figure 6C). KEGG also showed that lysosomes were enriched substantially (Figure 6B). The most remarkably altered proteins in CH versus C were involved in mitochondrial electron transport (Ndufs8, Coq9), lysosome organization (Tmem106b, Gba), and mitochondrion protein (Cmc2, Table S2). The hub genes were associated with apolipoprotein (Figure 6D).

3.4. Functional Correlation Analysis of DEPs in an HFD. Five DEPs were downregulated in the HE group compared with the HC group (Figure 7A). The enriched GO terms included mitochondrial electron transport, aerobic electron transport chain, and aerobic respiration (Figure 7B). The most remarkably altered proteins in HE versus HC were involved in ATPase activity (Hspe1, Tor3a), mitochondrial electron transport (Cox6c2), and cell adhesion (Cd44, Table S3).

A total of 71 upregulated and 17 downregulated DEPs were identified in the HH group compared with the HC group (Figure 8A). GO function annotation analysis showed that the DEPs affected by HIIT were related to Golgi (Figure 8C). KEGG also showed that lysosomes were enriched remarkably (Figure 8B). The most substantially altered proteins in HH versus HC were involved in immune response (Ig-like domain-containing protein), regulation of calcium ion transport (Cacna2d1, Ank2), and autophagosome (Tbc1d12, Atg12; Table S4). Unfortunately, many hub gene functions still need to be explored.

3.5. Response of Different Nutritional States to Exercise. The nutrition-induced effects of exercise on the proteome of AT were determined. A total of 139 and 5 DEPs were identified in CE versus C and HE versus HC, respectively. However, no common DEP was found between the two kinds of states (Figure 9A).
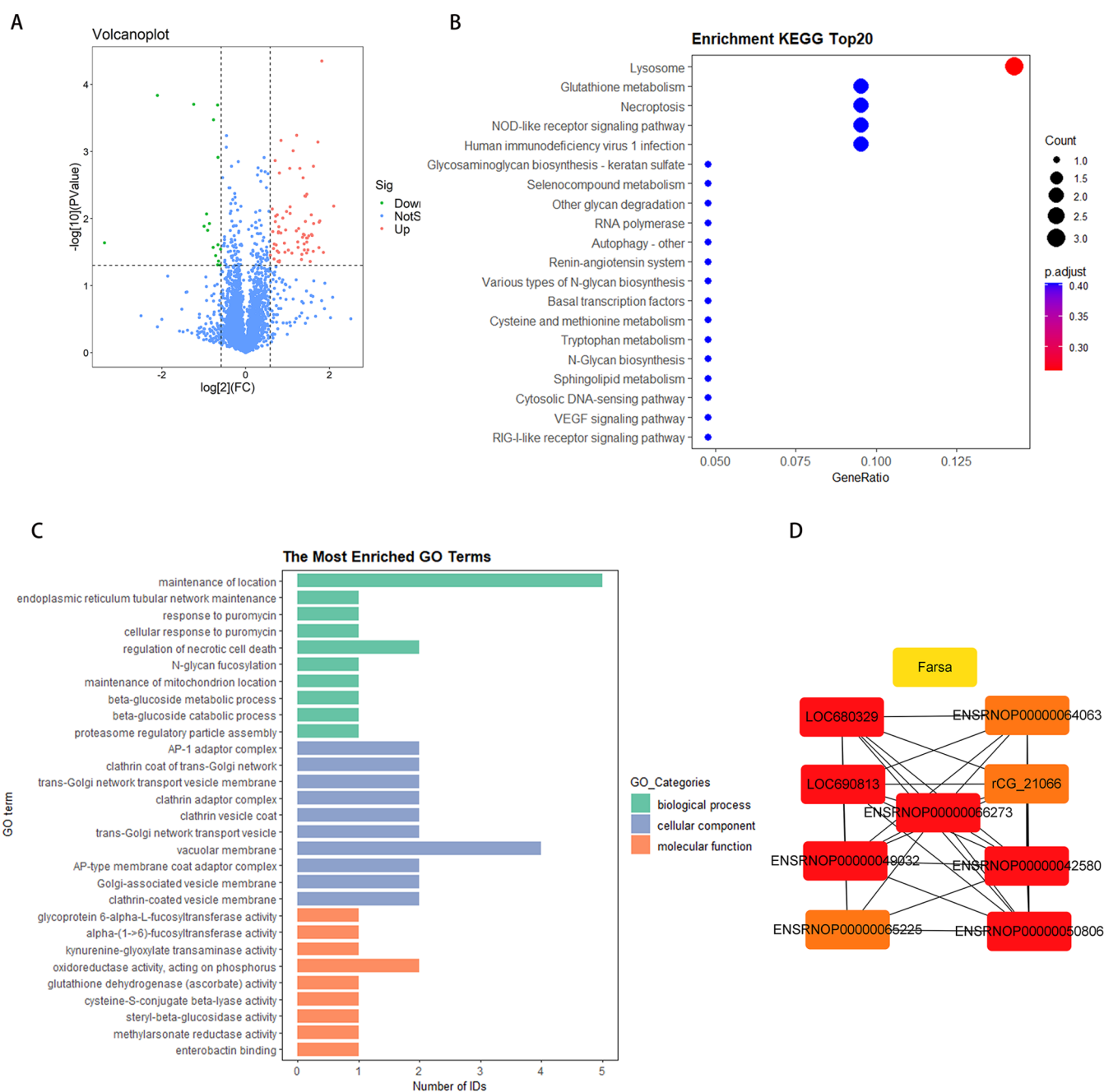
Figure 8. Functional correlation analysis of DEPs in HH versus HC. (A) Volcano map of DEPs in HH versus HC. (B) KEGG analysis in HH versus HC. (C) GO function annotation analysis in HH versus HC. (D) Top 10 hub genes of PPI in HH versus HC. The redder the color, the higher the MCC score.

A total of 204 and 88 DEPs were identified in CH versus C and HH versus HC, respectively. The two nutritional states had 22 common DEPs (Figure 9B). Functional analysis showed that the 22 common DEPs were enriched in the GO terms, pyridoxal phosphate binding, maintenance of location, maintenance of mitochondrion location, and respiratory electron transport chain, and 182 (except 22 common proteins) DEPs in CH versus C were enriched in the GO terms, phospholipid efflux, oxygen transport, and oxygen carrier activity. Sixty-six DEPs (except 22 common proteins) in HH versus HC were enriched in the GO terms, positive regulation of autophagy and RNA polymerase II.

3.6. Exercise Training Did Not Reverse the Effects of HFD on AT. A total of 27 DEPs were found in HC versus C,

including seven upregulated and seven downregulated proteins. The enrichment analyses of GO and KEGG showed that HFD caused the abnormal expression of lipid metabolism proteins, such as those related to cholesterol metabolism, fat digestion, and absorption (Figure 10). The related downregulated proteins included Apoa1, Apoa2, and Apoa4. MICT did not reverse the trend of protein expression induced by HFD. HIIT reversed the trend of nine protein expression induced by HFD, and six Ig-like domain-containing proteins were upregulated.

3.7. Protein Expression Levels of Enrichment Pathways in Different Groups. Based on the enrichment analysis results of GSEA and DEPs, we have listed the original data of some proteins. The following figure shows some key results (Figure 11).
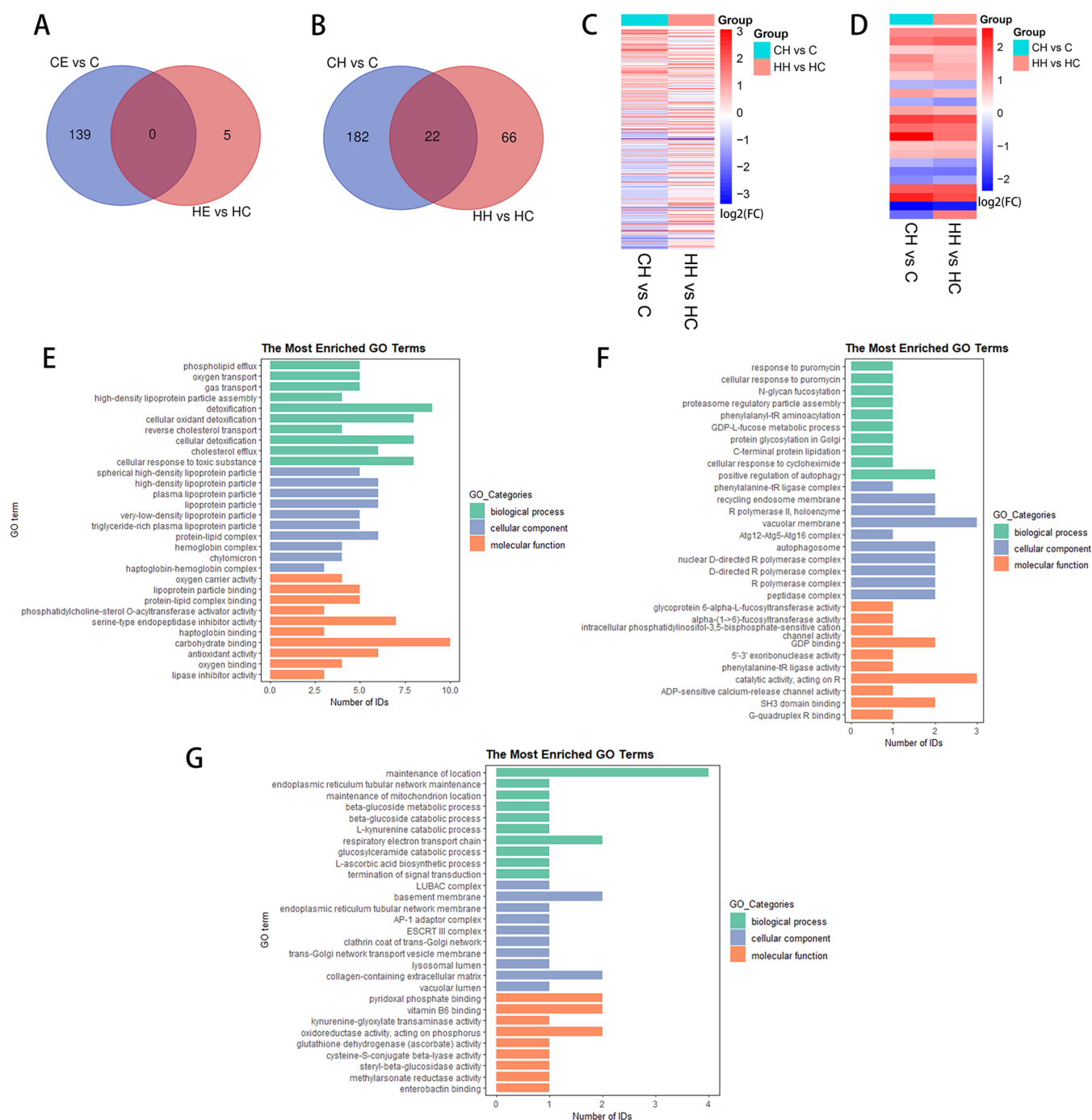
Figure 9. Differential effects of exercise in two nutritional states. (A) Venn diagram of CE versus C and HE versus HC. (B) Venn diagram of CH versus C and HH versus HC. (C) Heatmap of DEPs in CH versus C and HH vs HC. (D) Heatmap of common DEPs in CH versus C and HH versus HC, including 22 proteins. (E) GO terms enriched in CH versus C except 22 common DEPs. (F) GO terms enriched in HH versus HC except 22 common DEPs. (G) GO terms enriched in 22 common DEPs.

3.8. Proteomics Validation. To confirm whether differently expressed proteins were consistent with that determined by TMT-LC-MS/MS, we identified 3 of them (Figure 12). The relative expression levels of all of the proteins quantified by Western blot followed the trend of expression levels and significance determined by TMT quantification.

4. DISCUSSION

Although many proteomic studies on the effects of exercise on the body have been conducted, AT research is still scarce. A complete and comprehensive overview of the field is lacking because of the great variability of animal models, training programs, and other factors. AT is an important organ that reflects energy balance, and diet and exercise are important factors affecting energy balance.[23] Therefore, we carried out a study of the effects of diet and exercise on the proteomic characteristics of AT.

We observed that exercise from childhood promoted body skeletal muscle percentage and reduced body weight. HIIT and MICT activated ribosome, spliceosome, and the pentose phosphate pathway. Spliceosome, which affects RNA process-
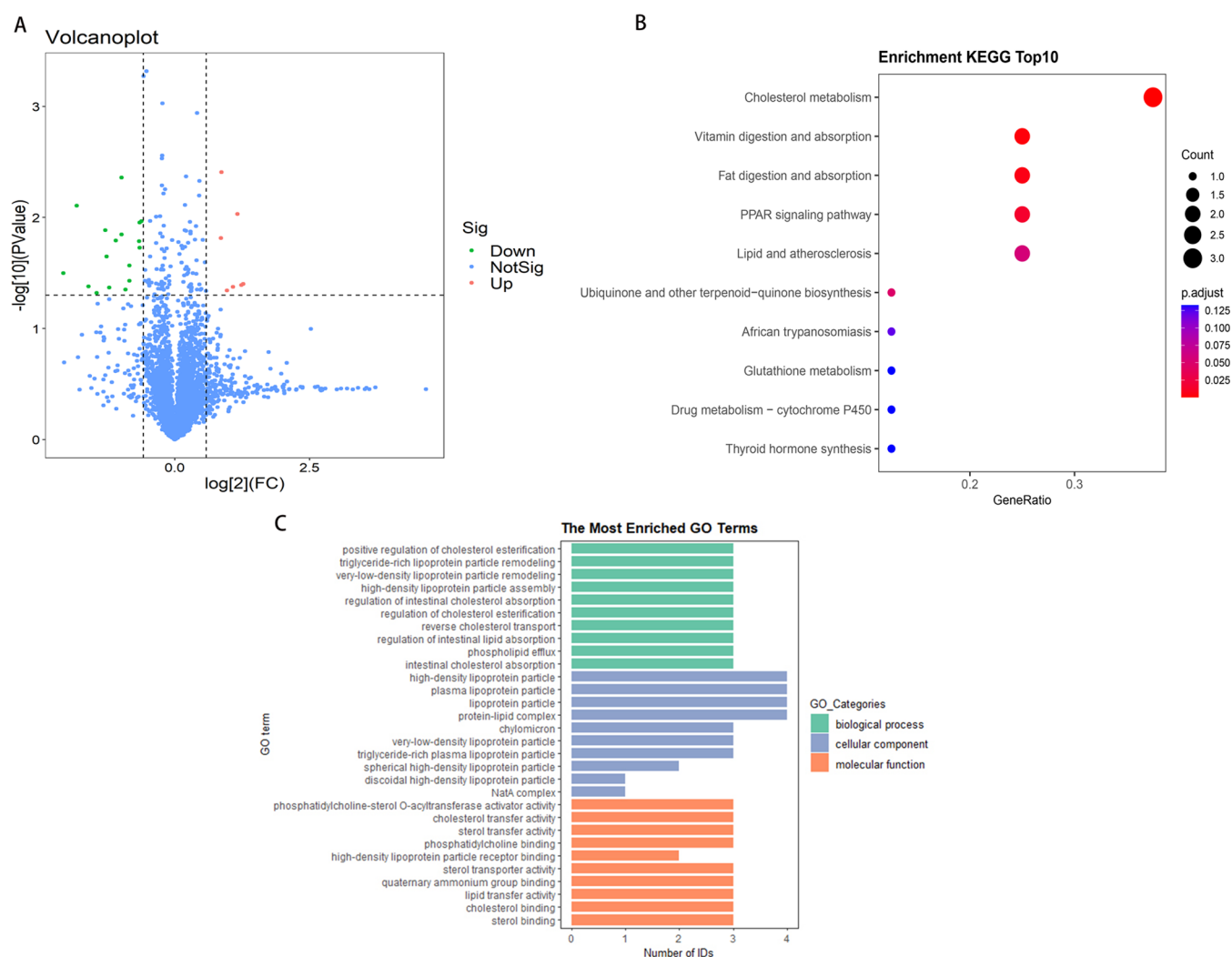
Figure 10. Functional correlation analysis of DEPs in HC versus C. (A) Volcano map of DEPs in HC versus C. (B) KEGG analysis in HC versus C. (C) GO function annotation analysis in HC versus C.

ing, plays an important role in protein diversity during development and adaptation.[24,25] It also affects AT production and thus has an effect on obesity; for example, knockdown of SRSF10 and SRSF2 adversely affects adipogenesis.[26−28] Our results showed that most splicing factors were increased in the exercise group, including SRSF10 and SRSF2, which might mean that the reduction in fat percentage could be detrimental. It may also be the body's resistance to stress response.[29] Physical activity affecting the spliceosome is recognized, but most studies are related to skeletal muscle.[30] Aldiss et al.[31] showed that rats swimming in thermoneutral water have a decreased expression of spliceosomes. Inconsistencies among training temperatures, training objects, and training programs may lead to inconsistent results. In any case, the role of the spliceosome in the influence of exercise on the body should be the direction of future research. A study of transcriptional profile in AT from healthy men with 6-month supervised exercise intervention identified pathways enriched in response to exercise, including the ribosome and proteasome.[32] Aldiss et al. also found that ribosomes play an important role in white AT through exercise training, but studies on related functions are still few. In addition, we need to acknowledge the importance of ribosomes in the field of sports, as they may compete with mitochondria in skeletal muscles.[33] The pentose phosphate pathway is a

fundamental component of cellular metabolism. It is important for maintaining carbon homeostasis, providing precursors for nucleotide and amino acid biosynthesis, providing reducing molecules for anabolism, and combating oxidative stress. DEPs showed that both modes of exercise were related to oxygen transport, and the expression of glycolytic protein Pfkp was significantly increased. HIIT involved the expression of HIF-1 pathway-related proteins and hypoxia-response-related pathways, which also suggested that HIIT is involved in the hypoxia-inducible environment. Some studies have shown that HIIT triggers the HIF-1 pathway in skeletal muscle,[34,35] but the effect on AT is still less. Our results showed that exercise boosts the body's metabolism.[36] Although the AT proteome and the ability to lose fat were somewhat similar between the two exercise modes, the proteomes affected by HIIT appeared to be concentrated in energy metabolism and biosynthesis, whereas the proteome affected by MICT was involved in the physiological function of protein and redox. Overall, exercise is beneficial because C-reactive protein (CRP) all declined after exercise, and its high expression is highly correlated with chronic metabolic diseases such as cardiovascular disease and diabetes.[37]

However, we found interesting results in HFD-fed rats that underwent exercise, which were reversed from the normal diet group. For example, opposite results existed for the expression of
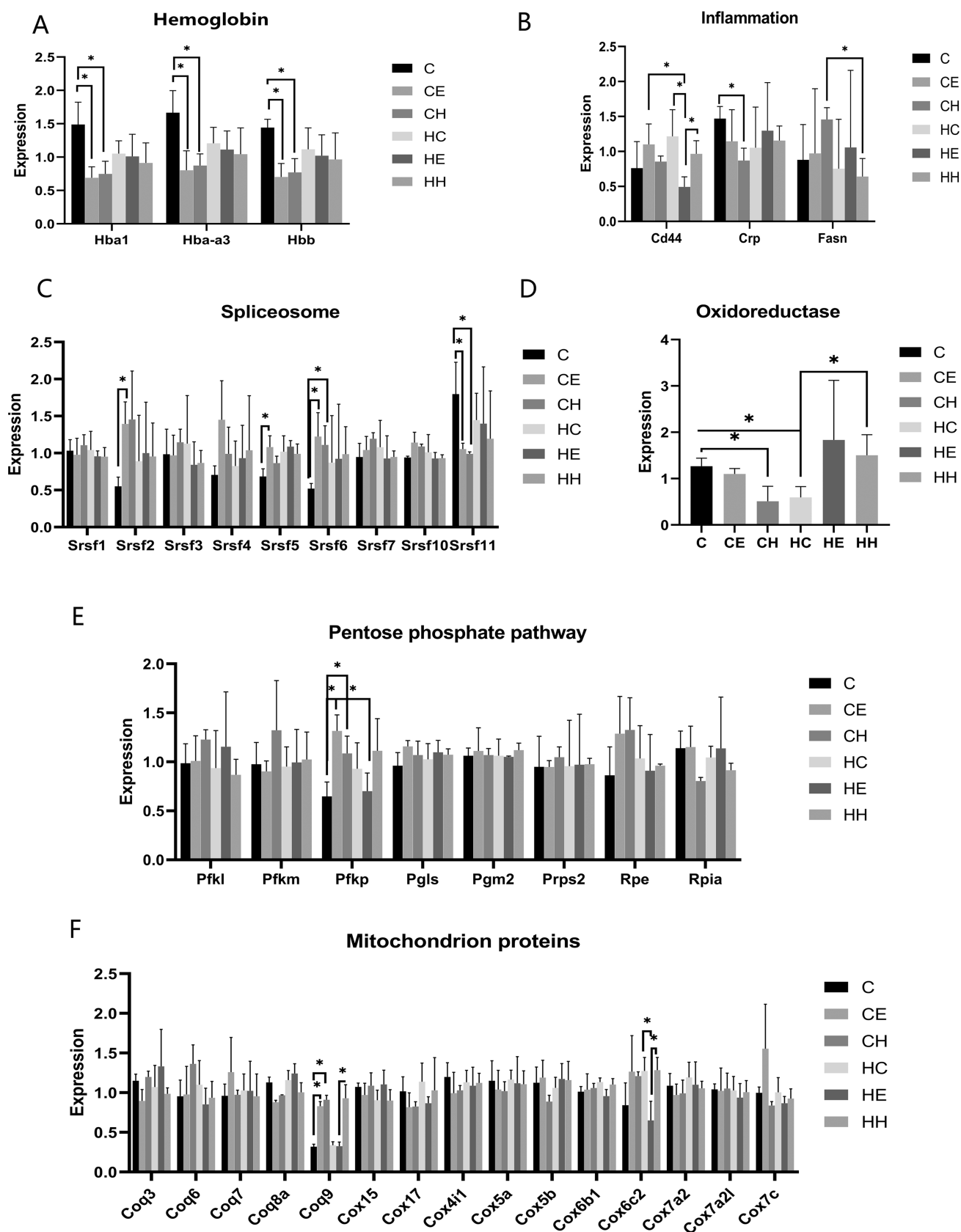
Figure 11. Protein expression levels of enrichment pathways in different groups. (A) Hemoglobin proteins, (B) inflammation, (C) spliceosome, (D) oxidoreductase, (E) pentose phosphate pathway, (F) mitochondrion proteins.

spliceosomes. In the case of HFD, a negative correlation exists between spliceosome expression and exercise. Therefore,

attention should be given to the effect of exercise on spliceosome. In HFD, the molecular response to HIIT seems
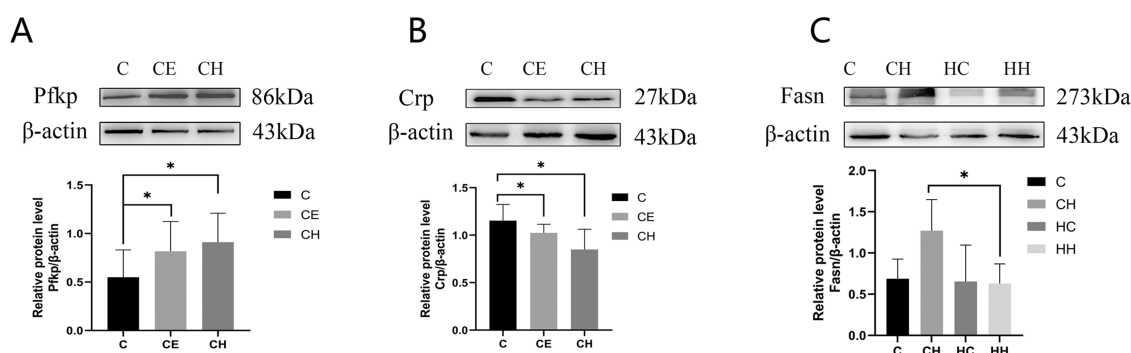
Figure 12. Results of Western blot. (A) Pfkp, (B) Crp, (C) Fasn.

to be stronger than that to MICT and affected more metabolic pathways and immune responses, although both modes of exercise can play a role in reducing fat and building muscle. Surprisingly, sWAT wet weight increased considerably when MICT was performed. Body fat percentage decreased; therefore, we reexamined the visceral AT data and found a remarkable decrease in visceral AT. Therefore, whether the increased sWAT content caused by MICT is an increase of "good fat" needs to be further explored.

In addition, the focus of our study was to understand the effects of exercise at different nutritional levels. Compared with normal diet, MICT with HFD affected the expression of a variety of mitochondrial proteins, whereas HIIT produced more immune stress proteins (about 35 kinds), such as immunoglobulin complex. During MICT, we did not find the same DEPs between the two nutritional states, suggesting that MICT responds differently to nutrition. Under normal diet, MICT affected various physiological processes and downregulated various hemoglobin genes (Hba1, Hba-a3, and Hbb) related to oxygen utilization. This result seems to be surprising. Whether the result means an increase in anaerobic metabolism still needs to be confirmed and explored in other tissues and organs. Some metabolism-related proteins that were downregulated by MICT in a high-fat state aroused our interest. For example, CD44 expression is elevated in obesity-induced white AT inflammation, and CD44 k/o mice are phenotypically healthier.[38] Our experiments observed that MICT with HFD led to a decrease in CD44, which seems to be a good performance. The cellular response to protein destruction is completed by the activation of heat shock proteins.[39] The E1 heat shock protein family (Hspe1) encodes Hspup0 protein, which is an important part of the Hsp60/Hspup0 system that assists in the folding of proteins in the mitochondrial matrix space.[40,41] HSPE1 in AT can be modulated by the neutrophil extracellular traps in obesity to increase inflammation.[42] Cox6c2 is the component of cytochrome c oxidase, the last enzyme in the mitochondrial electron transport chain that drives oxidative phosphorylation. Liver Cox6c2 decreases under a high-fat and high-cholesterol diet.[43] Although no AT-related data were obtained, the decrease in this protein caused by MICT with HFD needs to be considered.

When HIIT was performed, 22 proteins existed in both nutritional states. Although one protein whose expression trend was opposite, we speculated that the 21 proteins might be the key proteins of HIIT affecting AT remodeling and the expression trend of these proteins was not affected by diet. Some of these proteins were involved in the respiratory electron transport chain, such as Coq9. Coenzyme Q, also known as

ubiquinone, is a critical component of the mitochondrial electron transport chain. Coq9, which belongs to coenzyme Q, is a lipid-binding protein that can interact with Coq7 to enable coenzyme Q biosynthesis,[44] which affects cellular respiration and contributes to cellular anti-oxidation.[45] However, the role of this protein in AT still needs to be explored. The interacting proteins Cmc1 and Cmc2 act as a cytochrome c oxidase biogenesis factor to regulate mitochondrial superoxide dismutase activity, which plays an important role in cellular respiration and free radical scavenging.[46,47] A study[46] showed that the absence of Cmc2 induces a 5-fold increase in Cmc1 accumulation in yeast cell mitochondrial membranes. However, whether exercise causes the opposite expression of these two proteins in our study remains to be explored. Glutathione transferase omega (Gsto1), which is expressed oppositely in the two nutritional states, plays a pro-inflammatory role. A study showed that Gsto1−/− mice are less susceptible to HFD-induced obesity and AT inflammation.[48] However, in our study, Gsto1 was remarkably elevated in HIIT with HFD, suggesting a possible inflammatory response. Moreover, we analyzed the remaining proteins in each state except 22 proteins. The results showed that HIIT with normal diet also had the same decrease in hemoglobin genes (Hba-a1, Hba-a3, and Hbb) as MICT. We also noticed the downregulation of some lipoproteins, such as Apoa1, Apoa4, and Apom. This finding suggests that they are all beneficial circulating factors, which are also beneficial for obesity, insulin sensitivity, and atherosclerosis.[49−53] The result gives us a new hint that our HIIT regimen may have a certain negative impact on the molecular mechanisms of the organism, although we have obtained positive phenotypic effects. HIIT with HFD affected the positive regulation of autophagy, which upregulated Ras-related protein Rabup2 and two-pore calcium channel protein up (Tpc1). Rabup2 regulates mammalian/mechanistic target of rapamycin complex 1 activity and autophagy through the trafficking of PAT4, the initiation link of autophagy.[54] TPC1, which belongs to two-pore channels, participates in the regulation of multiple endolysosomal trafficking pathways; its knockdown can cause lysosomal dysfunction and affect metabolism.[55] Although HIIT resulted in positive phenotypic changes and some modest benefits at the molecular level in HFD, the resulting immune response was too strong. Whether this effect is beneficial still needs to be further explored in the future.

We observed that an HFD for 8 weeks resulted in changes in lipid metabolism and a remarkable increase in body fat percentage; therefore, we investigated whether exercise could reverse the adverse effects of HFD. From the proteomic level, we did not observe that exercise reversed the changes in protein

expression induced by HFD, and an increase in inflammation occurred during HIIT. However, in our study, we found individual differences in the effects of HFD on the body, which also led to some outliers in proteomic data. Such results are also related to the exercise intensity we chose. In spite of these factors, we still advocate a reasonable diet and exercise from the growth period to the maturity period according to the results.

We acknowledge that this work has several limitations. First, our sample size needs to be expanded, and further verification has not been done. Second, our exercise program is still relatively single, and HIIT has a variety of combinations; therefore, future studies should also explore HIIT with different intensities to obtain more comprehensive and objective data.

5. CONCLUSIONS AND SUGGESTIONS

The following conclusions were drawn from the results. The exercise stress response in the growing period was stronger and increased energy metabolism and metabolism, suggesting that exercise during the growing period should be appropriate. The two modes of exercise can reduce fat, increase muscle percentage, and improve maximum oxygen uptake in rats fed with HFD and trigger more immune responses in sWAT compared with rats with normal diet. Therefore, a reasonable diet and proper exercise should still be implemented. MICT is less likely to elicit the immune response of sWAT than HIIT in high-fat conditions. Spliceosomes may be the key factors in AT remodeling triggered by exercise and diet. Exercise may not fully reverse HFD-induced changes in protein expression. Although exercise is phenotypically beneficial, we advocate proper diet and exercise in the growth period.

Furthermore, our conclusions are not absolute. In the future, we still need to expand the sample size and change the exercise mode and intensity to further verify the results.

■ ASSOCIATED CONTENT

Data Availability Statement

The mass spectrometry proteomics data have been deposited to the ProteomeXchange Consortium (http://proteomecentral.proteomexchange.org) via the iProX partner repository[56,57] with the dataset identifier PXD041539.

Ⓢ Supporting Information

The Supporting Information is available free of charge at https://pubs.acs.org/doi/10.1021/acsomega.3c00627.

> Top 20 differentially regulated proteins in CE versus C (Table S1); Top 20 differentially regulated proteins in CH versus C (Table S2); Top 20 differentially regulated proteins in HE versus HC (Table S3); Top 20 differentially regulated proteins in HH versus HC (Table S4); and common differentially expressed proteins in CH versus C and HH versus HC (Table S5) (PDF)

■ AUTHOR INFORMATION

Corresponding Author

Yi Yan − *Department of Sport Biochemistry, School of Sport Science, Beijing Sport University, Beijing 100084, China; Laboratory of Sports Stress and Adaptation of General Administration of Sport, Beijing 100084, China; Laboratory of Physical Fitness and Exercise, Ministry of Education, Beijing Sport University, Beijing 100084, China;* ⓞ orcid.org/0000-0001-9904-7754; Email: yanyi@bsu.edu.cn

Authors

Ge Song − *Department of Sport Biochemistry, School of Sport Science, Beijing Sport University, Beijing 100084, China;* ⓞ orcid.org/0000-0002-1118-1850

Junying Chen − *Department of Sport Biochemistry, School of Sport Science, Beijing Sport University, Beijing 100084, China; Guangdong Ersha Sports Training Center, Guangzhou 510105, China*

Yimin Deng − *Department of Sport Biochemistry, School of Sport Science, Beijing Sport University, Beijing 100084, China; Fuzhou Medical College of Nanchang University, Fuzhou 344000, China*

Lingyu Sun − *Department of Sport Biochemistry, School of Sport Science, Beijing Sport University, Beijing 100084, China*

Complete contact information is available at:
https://pubs.acs.org/10.1021/acsomega.3c00627

Author Contributions

G.S. was responsible for the data collection, data interpretation, and writing and revision of the manuscript, under the direction and assistance of Y.Y. who assisted with each step and completion of the manuscript. J.C., Y.D., and L.S. were responsible for data collection.

Notes

The authors declare no competing financial interest.

■ ACKNOWLEDGMENTS

■ REFERENCES

(1) NCD Risk Factor Collaboration (NCD-RisC). Worldwide trends in body-mass index, underweight, overweight, and obesity from 1975 to 2016: a pooled analysis of 2416 population-based measurement studies in 1289 million children, adolescents, and adults. *Lancet* **2017**, *390*, 2627−2642.

(2) Escalon, H.; Courbet, D.; Julia, C.; Srour, B.; Hercberg, S.; Serry, A. J. Exposure of French Children and Adolescents to Advertising for Foods High in Fat, Sugar or Salt. *Nutrients* **2021**, *13*, No. 3741.

(3) Protudjer, J. L. P.; Marchessault, G.; Kozyrskyj, A. L.; Becker, A. B. Children's perceptions of healthful eating and physical activity. *Can. J. Diet Pract. Res.* **2010**, *71*, 19−23.

(4) Singh, A. S.; Mulder, C.; Twisk, J. W.; van Mechelen, W.; Chinapaw, M. J. Tracking of childhood overweight into adulthood: a systematic review of the literature. *Obes. Rev.* **2008**, *9*, 474−488.

(5) Janssen, I.; Leblanc, A. G. Systematic review of the health benefits of physical activity and fitness in school-aged children and youth. *Int. J. Behav. Nutr. Phys. Act.* **2010**, *7*, No. 40.

(6) Stoner, L.; Rowlands, D.; Morrison, A.; Credeur, D.; Hamlin, M.; Gaffney, K.; Lambrick, D.; Matheson, A. Efficacy of Exercise Intervention for Weight Loss in Overweight and Obese Adolescents: Meta-Analysis and Implications. *Sports Med.* **2016**, *46*, 1737−1751.

(7) Costa, E. C.; Hay, J. L.; Kehler, D. S.; Boreskie, K. F.; Arora, R. C.; Umpierre, D.; Szwajcer, A.; Duhamel, T. A. Effects of High-Intensity Interval Training Versus Moderate-Intensity Continuous Training On Blood Pressure in Adults with Pre- to Established Hypertension: A Systematic Review and Meta-Analysis of Randomized Trials. *Sports Med.* **2018**, *48*, 2127−2142.

(8) Groussard, C.; Maillard, F.; Vazeille, E.; Barnich, N.; Sirvent, P.; Otero, Y. F.; Combaret, L.; Madeuf, E.; Sourdrille, A.; Delcros, G.; et al.

Tissue-Specific Oxidative Stress Modulation by Exercise: A Comparison between MICT and HIIT in an Obese Rat Model. *Oxid. Med. Cell. Longev.* **2019**, *2019*, No. 1965364.

(9) Ramos, J. S.; Dalleck, L. C.; Tjonna, A. E.; Beetham, K. S.; Coombes, J. S. The impact of high-intensity interval training versus moderate-intensity continuous training on vascular function: a systematic review and meta-analysis. *Sports Med.* **2015**, *45*, 679−692.

(10) Wewege, M.; van den Berg, R.; Ward, R. E.; Keech, A. The effects of high-intensity interval training vs. moderate-intensity continuous training on body composition in overweight and obese adults: a systematic review and meta-analysis. *Obes. Rev.* **2017**, *18*, 635−646.

(11) Unamuno, X.; Fruhbeck, G.; Catalan, V. Adipose Tissue. In *Encyclopedia of Endocrine Diseases*, 2nd ed.; Huhtaniemi, I.; Martini, L., Eds.; Academic Press: Oxford, 2019; pp 370−384.

(12) Booth, A. D.; Magnuson, A. M.; Fouts, J.; Wei, Y.; Wang, D.; Pagliassotti, M. J.; Foster, M. T. Subcutaneous adipose tissue accumulation protects systemic glucose tolerance and muscle metabolism. *Adipocyte* **2018**, *7*, 261−272.

(13) Cox-York, K.; Wei, Y.; Wang, D.; Pagliassotti, M. J.; Foster, M. T. Lower body adipose tissue removal decreases glucose tolerance and insulin sensitivity in mice with exposure to high fat diet. *Adipocyte.* **2015**, *4*, 32−43.

(14) Foster, M. T.; Softic, S.; Caldwell, J.; Kohli, R.; de Kloet, A. D.; Seeley, R. J. Subcutaneous Adipose Tissue Transplantation in Diet-Induced Obese Mice Attenuates Metabolic Dysregulation While Removal Exacerbates It. *Physiol Rep.* **2013**, *1*, No. e00015.

(15) Gealekman, O.; Guseva, N.; Hartigan, C.; Apotheker, S.; Gorgoglione, M.; Gurav, K.; Tran, K. V.; Straubhaar, J.; Nicoloro, S.; Czech, M. P.; et al. Depot-specific differences and insufficient subcutaneous adipose tissue angiogenesis in human obesity. *Circulation* **2011**, *123*, 186−194.

(16) Palou, A.; Picó, C.; Bonet, M. L. Nutritional potential of metabolic remodelling of white adipose tissue. *Curr. Opin. Clin. Nutr. Metab. Care* **2013**, *16*, 650−656.

(17) Garritson, J. D.; Boudina, S. The Effects of Exercise on White and Brown Adipose Tissue Cellularity, Metabolic Activity and Remodeling. *Front. Physiol.* **2021**, *12*, No. 772894.

(18) Ahn, C.; Ryan, B. J.; Schleh, M. W.; Varshney, P.; Ludzki, A. C.; Gillen, J. B.; Van Pelt, D. W.; Pitchford, L. M.; Howton, S. M.; Rode, T.; et al. Exercise training remodels subcutaneous adipose tissue in adults with obesity even without weight loss. *J. Physiol.* **2022**, *600*, 2127−2146.

(19) Plubell, D. L.; Wilmarth, P. A.; Zhao, Y.; Fenton, A. M.; Minnier, J.; Reddy, A. P.; Klimek, J.; Yang, X.; David, L. L.; Pamir, N. Extended Multiplexing of Tandem Mass Tags (TMT) Labeling Reveals Age and High Fat Diet Specific Proteome Changes in Mouse Epididymal Adipose Tissue. *Mol. Cell Proteomics* **2017**, *16*, 873−890.

(20) Ayoub, H. M.; McDonald, M. R.; Sullivan, J. A.; Tsao, R.; Meckling, K. A. Proteomic Profiles of Adipose and Liver Tissues from an Animal Model of Metabolic Syndrome Fed Purple Vegetables. *Nutrients* **2018**, *10*, 456.

(21) Wang, F.; Chen, S.; Ren, L.; Wang, Y.; Li, Z.; Song, T.; Zhang, H.; Yang, Q. The Effect of Silibinin on Protein Expression Profile in White Adipose Tissue of Obese Mice. *Front. Pharmacol.* **2020**, *11*, 55.

(22) Landry, B. W.; Driscoll, S. W. Physical activity in children and adolescents. *PM&R* **2012**, *4*, 826−832.

(23) Atakan, M. M.; Koşar, N.; Güzel, Y.; Tin, H. T.; Yan, X. The Role of Exercise, Diet, and Cytokines in Preventing Obesity and Improving Adipose Tissue. *Nutrients* **2021**, *13*, No. 1459.

(24) Stamm, S.; Ben-Ari, S.; Rafalska, I.; Tang, Y.; Zhang, Z.; Toiber, D.; Thanaraj, T. A.; Soreq, H. Function of alternative splicing. *Gene* **2005**, *344*, 1−20.

(25) Nilsen, T. W.; Graveley, B. R. Expansion of the eukaryotic proteome by alternative splicing. *Nature* **2010**, *463*, 457−463.

(26) Lin, J. C. Impacts of Alternative Splicing Events on the Differentiation of Adipocytes. *Int. J. Mol. Sci.* **2015**, *16*, 22169−22189.

(27) Sánchez-Ceinos, J.; Guzmán-Ruiz, R.; Rangel-Zúñiga, O. A.; López-Alcalá, J.; Moreno-Caño, E.; Del Río-Moreno, M.; Romero-Cabrera, J. L.; Pérez-Martínez, P.; Maymo-Masip, E.; Vendrell, J.; et al. Impaired mRNA splicing and proteostasis in preadipocytes in obesity-related metabolic disease. *eLife* **2021**, *10*, No. e65996.

(28) Li, H.; Cheng, Y.; Wu, W.; Liu, Y.; Wei, N.; Feng, X.; Xie, Z.; Feng, Y. SRSF10 regulates alternative splicing and is required for adipocyte differentiation. *Mol. Cell. Biol.* **2014**, *34*, 2198−2207.

(29) Shkreta, L.; Delannoy, A.; Salvetti, A.; Chabot, B. SRSF10: an atypical splicing regulator with critical roles in stress response, organ development, and viral replication. *RNA* **2021**, *27*, 1302−1317.

(30) Ubaida-Mohien, C.; Gonzalez-Freire, M.; Lyashkov, A.; Moaddel, R.; Chia, C. W.; Simonsick, E. M.; Sen, R.; Ferrucci, L. Physical Activity Associated Proteomics of Skeletal Muscle: Being Physically Active in Daily Life May Protect Skeletal Muscle From Aging. *Front. Physiol.* **2019**, *10*, 312.

(31) Aldiss, P.; Lewis, J. E.; Lupini, I.; Bloor, I.; Chavoshinejad, R.; Boocock, D. J.; Miles, A. K.; Ebling, F. J. P.; Budge, H.; Symonds, M. E. Exercise Training in Obese Rats Does Not Induce Browning at Thermoneutrality and Induces a Muscle-Like Signature in Brown Adipose Tissue. *Front. Endocrinol.* **2020**, *11*, 97.

(32) Rönn, T.; Volkov, P.; Tornberg, A.; Elgzyri, T.; Hansson, O.; Eriksson, K. F.; Groop, L.; Ling, C. Extensive changes in the transcriptional profile of human adipose tissue including genes involved in oxidative phosphorylation after a 6-month exercise intervention. *Acta Physiol.* **2014**, *211*, 188−200.

(33) Mesquita, P. H. C.; Vann, C. G.; Phillips, S. M.; McKendry, J.; Young, K. C.; Kavazis, A. N.; Roberts, M. D. Skeletal Muscle Ribosome and Mitochondrial Biogenesis in Response to Different Exercise Training Modalities. *Front. Physiol.* **2021**, *12*, No. 725866.

(34) Abe, T.; Kitaoka, Y.; Kikuchi, D. M.; Takeda, K.; Numata, O.; Takemasa, T. High-intensity interval training-induced metabolic adaptation coupled with an increase in Hif-1α and glycolytic protein expression. *J. Appl. Physiol.* **2015**, *119*, 1297−1302.

(35) Holloway, T. M.; Bloemberg, D.; Da, S. M.; Quadrilatero, J.; Spriet, L. L. High-intensity interval and endurance training are associated with divergent skeletal muscle adaptations in a rodent model of hypertension. *Am. J. Physiol. Regul. Integr. Comp. Physiol.* **2015**, *308*, R927−R934.

(36) Stincone, A.; Prigione, A.; Cramer, T.; Wamelink, M. M.; Campbell, K.; Cheung, E.; Olin-Sandoval, V.; Grüning, N. M.; Krüger, A.; Tauqeer Alam, M.; et al. The return of metabolism: biochemistry and physiology of the pentose phosphate pathway. *Biol. Rev. Camb. Philos. Soc.* **2015**, *90*, 927−963.

(37) Yudkin, J. S.; Stehouwer, C. D.; Emeis, J. J.; Coppack, S. W. C-reactive protein in healthy subjects: associations with obesity, insulin resistance, and endothelial dysfunction: a potential role for cytokines originating from adipose tissue? *Arterioscler., Thromb., Vasc. Biol.* **1999**, *19*, 972−978.

(38) Kang, H. S.; Liao, G.; DeGraff, L. M.; Gerrish, K.; Bortner, C. D.; Garantziotis, S.; Jetten, A. M. CD44 plays a critical role in regulating diet-induced adipose inflammation, hepatic steatosis, and insulin resistance. *Plos One* **2013**, *8*, No. e58417.

(39) Lang, B. J.; Guerrero, M. E.; Prince, T. L.; Okusha, Y.; Bonorino, C.; Calderwood, S. K. The functions and regulation of heat shock proteins; key orchestrators of proteostasis and the heat shock response. *Arch. Toxicol.* **2021**, *95*, 1943−1970.

(40) Hartman, D. J.; Hoogenraad, N. J.; Condron, R.; Høj, P. B. Identification of a mammalian 10-kDa heat shock protein, a mitochondrial chaperonin 10 homologue essential for assisted folding of trimeric ornithine transcarbamoylase in vitro. *Proc. Natl. Acad. Sci. U.S.A.* **1992**, *89*, 3394−3398.

(41) Cheng, M. Y.; Hartl, F. U.; Martin, J.; Pollock, R. A.; Kalousek, F.; Neupert, W.; Hallberg, E. M.; Hallberg, R. L.; Horwich, A. L. Mitochondrial heat-shock protein hsp60 is essential for assembly of proteins imported into yeast mitochondria. *Nature* **1989**, *337*, 620−625.

(42) Freitas, D. F.; Colón, D. F.; Silva, R. L.; Santos, E. M.; Guimarães, V.; Ribeiro, G.; de Paula, A. M. B.; Guimarães, A. L. S.; Dos Reis, S. T.; Cunha, F. Q.; et al. Neutrophil extracellular traps (NETs) modulate inflammatory profile in obese humans and mice: adipose tissue role on NETs levels. *Mol. Biol. Rep.* **2022**, *49*, 3225−3236.

(43) You, Y.; Zhang, Y.; Lu, Y.; Hu, K.; Qu, X.; Liu, Y.; Lu, B.; Jin, L. Protein profiling and functional analysis of liver mitochondria from rats with nonalcoholic steatohepatitis. *Mol. Med. Rep.* **2017**, *16*, 2379−2388.

(44) Lohman, D. C.; Forouhar, F.; Beebe, E. T.; Stefely, M. S.; Minogue, C. E.; Ulbrich, A.; Stefely, J. A.; Sukumar, S.; Luna-Sánchez, M.; Jochem, A.; et al. Mitochondrial COQ9 is a lipid-binding protein that associates with COQ7 to enable coenzyme Q biosynthesis. *Proc. Natl. Acad. Sci. U.S.A.* **2014**, *111*, E4697−E4705.

(45) Turunen, M.; Olsson, J.; Dallner, G. Metabolism and function of coenzyme Q. *Biochim. Biophys. Acta, Biomembr.* **2004**, *1660*, 171−199.

(46) Horn, D.; Zhou, W.; Trevisson, E.; Al-Ali, H.; Harris, T. K.; Salviati, L.; Barrientos, A. The conserved mitochondrial twin Cx9C protein Cmc2 Is a Cmc1 homologue essential for cytochrome c oxidase biogenesis. *J. Biol. Chem.* **2010**, *285*, 15088−15099.

(47) Watson, S. A.; McStay, G. P. Functions of Cytochrome c oxidase Assembly Factors. *Int. J. Mol. Sci.* **2020**, *21*, No. 7254.

(48) Menon, D.; Innes, A.; Oakley, A. J.; Dahlstrom, J. E.; Jensen, L. M.; Brüstle, A.; Tummala, P.; Rooke, M.; Casarotto, M. G.; Baell, J. B.; et al. GSTO1-1 plays a pro-inflammatory role in models of inflammation, colitis and obesity. *Sci. Rep.* **2017**, *7*, No. 17832.

(49) Tavernier, G.; Caspar-Bauguil, S.; Viguerie, N. Apolipoprotein M: new connections with diet, adipose tissue and metabolic syndrome. *Curr. Opin. Lipidol.* **2020**, *31*, 8−14.

(50) Frances, L.; Tavernier, G.; Viguerie, N. Adipose-Derived Lipid-Binding Proteins: The Good, the Bad and the Metabolic Diseases. *Int J Mol Sci.* **2021**, *22*, No. 10460.

(51) Kalogeropoulou, C.; Hatziri, A.; Xepapadaki, E.; Savvoulidou, O.; Karavia, E. A.; Zvintzou, E.; Constantinou, C.; Kypreos, K. E. Isoform and tissue dependent impact of apolipoprotein E on adipose tissue metabolic activation: The role of apolipoprotein A1. *Biochim. Biophys. Acta, Mol. Cell Biol. Lipids* **2020**, *1865*, No. 158551.

(52) Ruan, X.; Li, Z.; Zhang, Y.; Yang, L.; Pan, Y.; Wang, Z.; Feng, G. S.; Chen, Y. Apolipoprotein A-I possesses an anti-obesity effect associated with increase of energy expenditure and up-regulation of UCP1 in brown fat. *J. Cell. Mol. Med.* **2011**, *15*, 763−772.

(53) Qu, J.; Ko, C. W.; Tso, P.; Bhargava, A. Apolipoprotein A-IV: A Multifunctional Protein Involved in Protection against Atherosclerosis and Diabetes. *Cells* **2019**, *8*, No. 319.

(54) Matsui, T.; Fukuda, M. Rab12 regulates mTORC1 activity and autophagy through controlling the degradation of amino-acid transporter PAT4. *Embo Rep.* **2013**, *14*, 450−457.

(55) Grimm, C.; Chen, C. C.; Wahl-Schott, C.; Biel, M. Two-Pore Channels: Catalyzers of Endolysosomal Transport and Function. *Front. Pharmacol.* **2017**, *08*, 45.

(56) Ma, J.; Chen, T.; Wu, S.; Yang, C.; Bai, M.; Shu, K.; Li, K.; Zhang, G.; Jin, Z.; He, F.; Hermjakob, H.; Zhu, Y. iProX: an integrated proteome resource. *Nucleic Acids Res.* **2019**, *47*, D1211−D1217.

(57) Chen, T.; Ma, J.; Liu, Y.; Chen, Z.; Xiao, N.; Lu, Y.; Fu, Y.; Yang, C.; Li, M.; Wu, S.; Wang, X.; Li, D.; He, F.; Hermjakob, H.; Zhu, Y. iProX in 2021: connecting proteomics data sharing with big data. *Nucleic Acids Res.* **2022**, *50*, D1522−D1527.